**REFERENCES**

1. **Schultz, E. and K.M. McCormick.** 1994. Skeletal muscle satellite cells. Rev. Phys. Biochem. Pharm. *123*:213-257.
2. **Hartley, R.S., E. Bandman, and Z. Yablonka-Reuveni.** 1992. Skeletal muscle satellite cells appear during late chicken embryogenesis. Dev. Bio. *153*:206-216.
3. **Campion, D.R.** 1984.The muscle satellite cell: a review. Int. Rev. Cytol. *87*:225-251.
4. **Asakura, A., M. Komaki, and M.A. Rudnicki.** 2001. Muscle satellite cells are multipotential stem cells that exhibit myogenic, osteogenic, and adipogenic differentiation. Differentiation *68*:245-253.
5. **Stockdale, F.E. and H. Holtzer.** 1961. DNA synthesis and myogenesis. Exp. Cell Res. *24*: 508-520.
6. **McCormick, K.M. and E. Schultz.** 1992. Mechanisms of nascent fiber formation during avian skeletal muscle hypertrophy. J. Appl. Physiol. *72*:888-893.
7. **Mozdziak, P.E., T. Fassel, R. Gregory, E. Schultz, M.L. Greaser, and R.G. Cassens.** 1994. Quantitation of satellite cell proliferation in vivo using image analysis. Biotech. Histochem. *69*:249-252.
8. **Mozdziak, P.E., E. Schultz, and R.G. Cassens.** 1994. Satellite cell mitotic activity during turkey skeletal muscle growth. Poult. Sci. *73*:547-555.
9. **Applegate, T.J., J.J. Dibner, M.L. Kitchell, Z. Uni, and M.S. Lilburn.** 1999. Effect of turkey (*Meleagridis gallopavo*) breeder hen age and egg size on poult development. 2. Intestinal villus growth, enterocyte migration and proliferation of the turkey poult. Comp. Bio. Physio. B *124*:381-389.
10. **Moss, F.P. and C.P. Leblond.** 1971. Satellite cells as the source of nuclei in muscles of growing rats. Anat. Rec. *170*:421-435.
11. **Schultz, E.** 1996. Satellite cell proliferative compartments in growing skeletal muscle. Dev. Biol. *175*:84-94.
12. **Swartz, D.R., M.L. Greaser, and B.B. Marsh.** 1990. Regulation of binding of subfragment 1 in isolated rigor myofibrils. J. Cell Bio. *111*: 2989-3001.
13. **Hamburger, V. and H.L. Hamilton.** 1951. A series of normal stages in the development of the chick embryo. J. Morphol. *88*:49-92.
14. **Giamario, C., J.N. Petite, and P.E. Mozdziak.** 2003. Hatchability of chicken embryos following somite manipulation. BioTechniques 34: 1128-1130.


Received 24 September 2003; accepted 9 October 2003.

*Address correspondence to Paul Mozdziak, North Carolina State University, Department of Poultry Science, Campus Box 7608/Scott Hall, Raleigh, NC 27695, USA. e-mail: pemozdzi@unity.ncsu.edu*

# Comparison of RiboGreen® and 18S rRNA quantitation for normalizing real-time RT-PCR expression analysis

Joel G. Hashimoto, Amy S. Beadles-Bohling, and Kristine M. Wiren
*Oregon Health & Science University, Portland, OR, USA*

*BioTechniques 36:54-60 (January 2004)*

Real-time RT-PCR is becoming the method of choice for monitoring or confirming mRNA expression (1–3). With unparalleled sensitivity, the ability to use 100 to 1000 times less RNA than other methodologies, and high-throughput potential for gene discovery approaches, real-time RT-PCR gives researchers the ability to determine mRNA abundance quickly and efficiently (1,4). While Northern blot analysis remains the most accepted method for measuring mRNA abundance, there are drawbacks that limit its utility. First, Northern blot analysis requires several micrograms of total RNA for each lane, which precludes the analysis of microdissected samples, tissue from laser capture, or other valuable samples due to the high cost and/or inability to obtain sufficient amounts of RNA. Second, Northern analysis is limited by the number of samples that can be run simultaneously on a gel, or requires standard or control samples on each blot for normalization between other Northern blots. Finally, the limited sensitivity of Northern analysis, given the indirect nature of the measurement and the multiple steps required, necessitates a robust change in the abundance of a given transcript to obtain a statistically significant result.

All methods of RNA quantification rely on normalization methods to quantitatively compare multiple disparate samples. Due to the sensitivity of the assay, real-time RT-PCR requires accurate methods for normalizing both for the amount of RNA added to each reaction and for reaction efficiency (1,4). Standard methods used for normalization of RNA amounts include analysis of absorbance at 260 nm, or real-time RT-PCR analysis of housekeeping genes or 18S rRNA abundance (1). Absorbance at 260 nm is the most problematic approach because a large amount of RNA is required, samples will necessarily be subsequently diluted, and contaminates that are present in the sample frequently adversely influence the accuracy of the quantifications. Housekeeping genes are suitable for normalization in some cases, but require additional analysis to verify the specific treatment or experimental conditions do not alter their steady-state mRNA abundance (1).

The use of 18S rRNA abundance for normalization in real-time RT-PCR analysis has been effective in our hands. Advantages include the fact that 18S rRNA has a low turnover rate and the large 18S rRNA pool is less prone to substantial changes from physiological perturbations. However, there are both technical and logistical limitations to its utility. First, because 18S rRNA is much more abundant than any typical mRNA transcript (i.e., the large pool noted above), total RNA must be diluted to obtain a threshold value within the dynamic range of real-time PCR instruments, which inevitably introduces variability to the measurement. Second, running samples an additional time to obtain normalization values for each sample leads to cost considerations, both in terms of supplies and setup time. Because of these limitations, we have developed an alternative normalization method using the RNA-specific fluorescent dye RiboGreen® (Molecular Probes, Eugene, OR, USA) (5) in conjunction with the iCycler iQ™ real-time PCR thermocycler (Bio-Rad Laboratories, Hercules, CA, USA). The method described here harnesses the sensitivity of the RiboGreen RNA assay for quantitation of RNA (5) and adapts the fluorescence excitation and

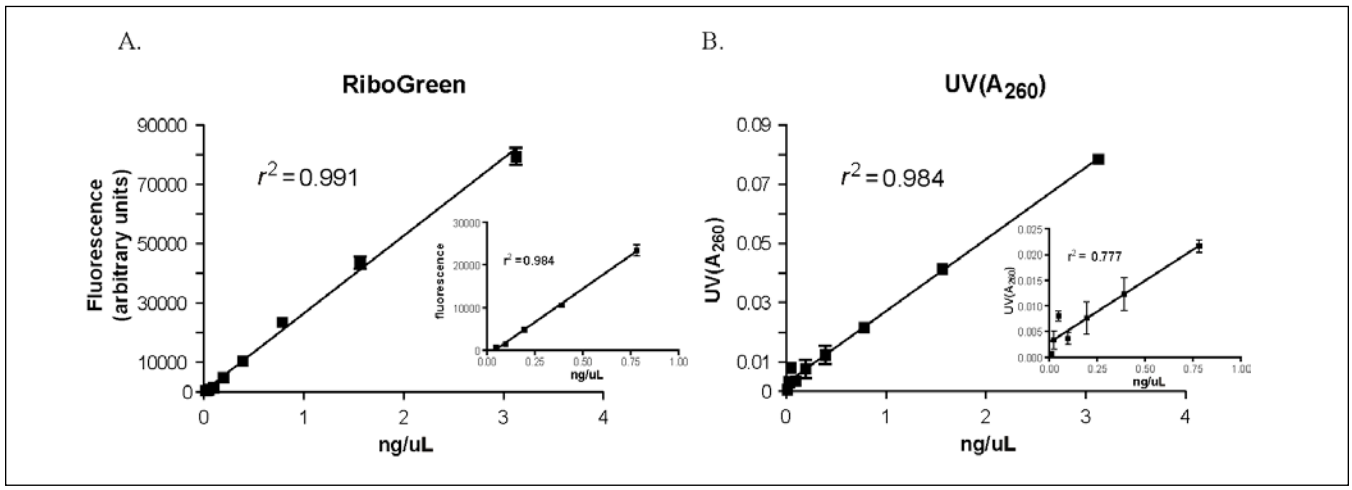


**Figure 1. Comparison of accuracy and dynamic range of RNA concentrations determined by (A) RiboGreen and (B) UV absorbance at 260 nm.** Both assays were performed on a twofold dilution series of the rRNA standard included in the RiboGreen kit. UV 260:280 ratios did not differ significantly from 2.0. At higher RNA concentrations, both assays perform similarly. At lower RNA concentrations (inset), the RiboGreen assay is more accurate and precise.

detection of a real-time PCR thermocycler to function as a 96-well fluorometer (6). The use of the optical thermocycler in this application results in more accurate and broadly applicable normalization, higher throughput, and decreased cost of real-time RT-PCR assays, and alleviates the need to purchase additional instrumentation to run the RiboGreen fluorometric assay.

Real-time RT-PCR and RiboGreen assays were carried out using the iCycler with the iQ Real-Time analysis module. Total RNA isolated with RNA STAT-60™ (Tel-Test, Friendswood, TX, USA) followed by DNase treatment was employed as template. One-step RT-PCR was carried out using the QuantiTect™ SYBR® Green I RT-PCR Kit (Qiagen, Valencia, CA, USA) according to the manufacturer's suggestions. Spectrophotometric analysis of the DNase-treated RNA showed RNA was free of contaminates as indicated by UV 260/280 ratios of 2.0. RT-PCRs were carried out in 25 µL volumes with 20 ng of total RNA for gene expression reactions and 100 pg of total RNA for 18S reactions. The following primers were used for the PCR amplifications: m5ard-F (5′-TGCGGTTTAGCGTCGGTGTC-3′); m5ard-R (5′-CCAAGTGGCCAAAGCGTA-3′); m18S-F (5′-GTTCCGACCATAAACGATGCC-3′); and m18S-R (5′-TGGTGGTGCCCTTCCGTCAAT-3′). Real-time RT-PCR efficiency was determined for each primer set using a fivefold dilution series of total RNA and did not differ significantly from 100%. Individual reaction kinetics were also analyzed to ensure each real-time RT-PCR did not differ significantly from 100% (3,7).

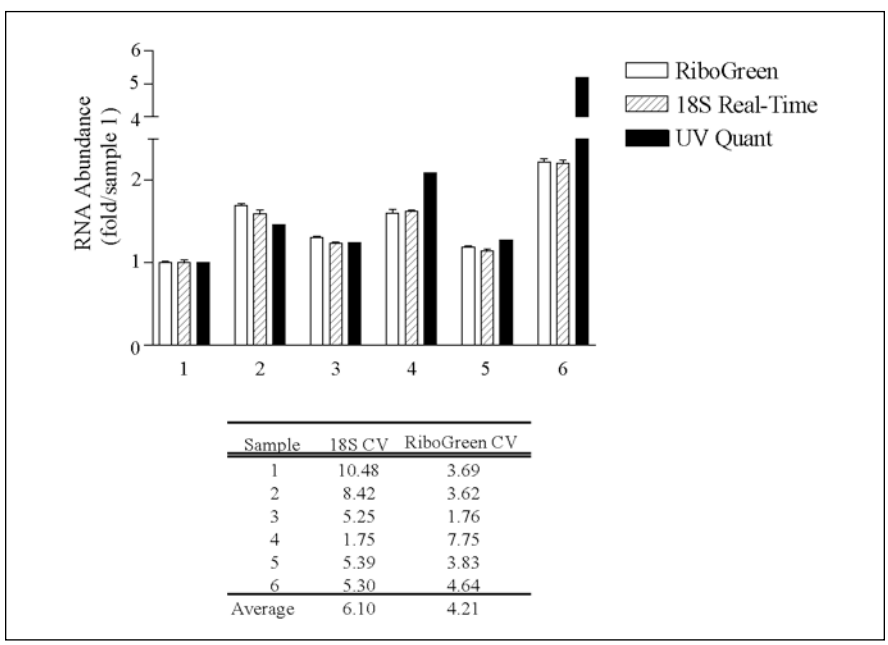


| Sample | 18S CV | RiboGreen CV |
|---|---|---|
| 1 | 10.48 | 3.69 |
| 2 | 8.42 | 3.62 |
| 3 | 5.25 | 1.76 |
| 4 | 1.75 | 7.75 |
| 5 | 5.39 | 3.83 |
| 6 | 5.30 | 4.64 |
| Average | 6.10 | 4.21 |

**Figure 2. Comparison of standard RNA quantification methods.** RiboGreen and 18S rRNA real-time RT-PCR data represent the mean of triplicate measurements ($\bar{x} \pm$ SEM). $UV_{260}$ data was used to calculate RNA concentrations, determined with a single measurement. UV 260:280 ratios did not differ significantly from 2.0. UV Quant, UV quantitation measured as absorbance at 260 nm; CV, coefficient of variation.

The RiboGreen RNA Quantitation Kit was employed as recommended by the manufacturer with the following modifications. An RNA standard curve was generated as a twofold serial dilution series ranging from 2000 pg/µL to 31.25 pg/µL in TE (10 mM Tris, 1 mM EDTA) buffer. For each experimental sample, 2 µL of the RNA aliquot used in the real-time RT-PCR was added to 98 µL of TE. Following the addition of 1 equivalent volume of 1× RiboGreen dye, three 50-µL aliquots of each standard, blank, and experimental sample were loaded individually into three adjacent wells of a 96-well PCR plate. Well factors were collected from an

external well factor plate containing 50 µL of a 1:10 dilution of the Bio-Rad External Well Factor Solution in each well of a 96-well PCR plate. The following iCyler protocol was used for fluorometer measurements: 1 min at 25°C and 6 cycles of 20 s at 25°C with fluorescence monitored during the final six cycles. After external well factor collection, the protocol was resumed and the iCycler block was allowed to cool to 25°C before pausing the protocol and adding the experimental 96-well plate.

Following the RiboGreen assay on the iCycler, raw fluorescence data was pasted into a Microsoft® Excel spreadsheet and an average fluorescence for each well and sample was calculated. After background fluorescence subtraction, fluorescence was converted to nanograms per well based on the RNA standard curve. Using a real-time RT-PCR standard curve generated from a fivefold dilution series of total RNA for mouse 5α-reductase (*Srd5a*1), the amount of total RNA loaded for each RT-PCR was converted into crossing thresholds [$C_t$], which were used along with the *Srd5a*1 $C_t$ to determine relative expression using the $\Delta\Delta C_t$ method (8). Fold regulation was then determined by normalizing all values to the mean of the relative expression for the control group and is presented as mean ($\bar{x} \pm$ SEM).

The linearity and dynamic range of RNA concentrations determined by absorbance at 260 nm and RiboGreen on a twofold serial dilution of the standard rRNA stock included in the RiboGreen kit are shown in Figure 1. At high RNA concentrations, absorbance at 260 nm and the RiboGreen assay are comparable. However, at RNA concentrations typically used for real-time RT-PCR assays, the RiboGreen assay clearly demonstrates less variability ($r^2 = 0.984$ vs. $r^2 = 0.777$) than UV absorbance for RNA quantification. Thus, the RiboGreen approach allows more accurate measurement of lower amounts of RNA. The ability of the RiboGreen method to assess total RNA abundance is compared to real-time RT-PCR for the 18S rRNA subunit and UV absorbance at 260 nm in Figure 2. The table of coefficient of variation values for each RNA sample indicates the RiboGreen assay has less overall variation when compared to 18S rRNA real-time RT-PCR. Normalization of real-time RT-PCR data for an mRNA transcript (5α-reductase mRNA) derived from three distinct mouse brain regions, using either 18S rRNA abundance or RiboGreen, is compared in Figure 3. The RiboGreen normalized data has a lower coefficient of variation than the 18S data in every case, indicating a clear benefit of using the RiboGreen assay to normalize real-time RT-PCR data for analysis of gene expression.

The ability to measure relative transcript abundance in samples of 10–20 ng of total RNA afforded by real-time RT-PCR analysis with SYBR Green I detection has created a cost-effective approach to research, both in terms of throughput volume and in the ability to resolve small but significant changes in increasingly small tissue samples (1,2,4). However, a continuing limitation to the application of this technolo-

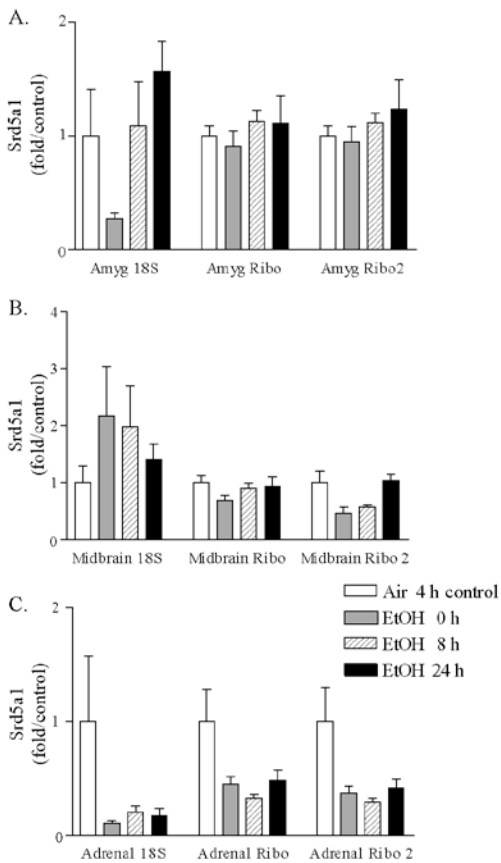


| | Amygdala | | | Midbrain | | | Adrenal | | |
|---|---|---|---|---|---|---|---|---|---|
| Sample | 18S CV | RiboGreenI CV | RiboGreenII CV | 18S CV | RiboGreenI CV | RiboGreenII CV | 18S CV | RiboGreenI CV | RiboGreenII CV |
| Air | 99.90 | 20.85 | 20.73 | 72.45 | 29.54 | 48.97 | 140.45 | 69.87 | 74.21 |
| EtOH 0hr | 43.69 | 37.07 | 34.91 | 97.65 | 30.11 | 55.81 | 53.60 | 35.17 | 41.95 |
| EtOH 8hr | 87.43 | 21.36 | 18.03 | 89.14 | 22.79 | 15.11 | 68.91 | 23.66 | 33.63 |
| EtOH 24hr | 41.35 | 52.49 | 51.72 | 47.82 | 46.71 | 25.67 | 88.94 | 45.80 | 42.35 |
| Average | 68.09 | 32.94 | 31.35 | 76.77 | 32.29 | 36.39 | 87.98 | 43.63 | 48.03 |

**Figure 3. Comparison of 18S rRNA normalized real-time RT-PCR data and RiboGreen normalized data for analysis of gene expression.** *Srd5a*1 (5α-reductase) mRNA abundance was determined in dissected mouse amygdala (A), midbrain (B), and adrenal gland (C) at various points of ethanol withdrawal. In all cases, RiboGreen normalized data shows lower or equivalent overall error compared to the 18S rRNA normalized data. Ribo2 represents a repeat of the RiboGreen assay to demonstrate the reproducibility of the assay. CV, coefficient of variation.

gy is the lack of any single "universal" gene to normalize transcript abundance to the amount of RNA loaded. While specific genes may be appropriate under certain experimental conditions, the absence of regulation must be confirmed in each case, slowing the time to discovery and increasing cost of analysis. The 18S rRNA gene has been used effectively for the normalization of real-time RT-PCR data but certain technical and throughput issues (i.e., multiple dilutions of total RNA and repetition of the real-time RT-PCR procedure for each sample to normalize, respectively) give reason to consider other normalization methods.

We have thus developed a novel application of the iQ real-time detection module of the iCycler thermocycler employing the RiboGreen assay (5) to quantify RNA concentrations down to several picograms per microliter. The RiboGreen assay is both far superior to and uses much less sample for analysis than UV absorbance at 260 nm (Figure 1). In addition, real-time RT-PCR data obtained for the example employed here, the 5α-reductase mRNA from various brain regions, showed similar or less error when normalized with results from the RiboGreen assay compared to real-time RT-PCR data for 18S rRNA (Figure 2 and 3). The reduced variation seen in the RiboGreen normalized data shown in Figure 2, and repeated with other mRNA species from different RNA samples (data not shown), is likely attributable to the dilutions required to assay for 18S rRNA from total RNA.

As normalization of real-time PCR data is required to correct for loading differences of template assuming individual reaction efficiencies have been determined to be similar, the use of a precise, accurate, and sensitive assay for determination of total RNA abundance is conceptually preferential to other methods such as housekeeping gene or 18S rRNA normalization (1,9). Not only does the use of RiboGreen to normalize real-time RT-PCR data reduce the cost of consumables and the amount of RNA required, the time that the iCycler is used is also reduced compared to assaying for both target and 18S rRNA in separate reactions. For example, an individual real-time RT-PCR reaction as previously described costs approximately $1.65, whereas an individual RiboGreen reaction costs approximately $0.08. A full 96-well real-time RT-PCR takes 2.5-3 h of machine time, while the RiboGreen assay uses approximately 20 min of machine time. The approach described here would be most advantageous when assaying the regulation of a small number of genes from a large number of different samples, but the trend toward reduced variability with the RiboGreen normalized data suggests it may be better in most applications for the determination of gene expression differences.

**ACKNOWLEDGMENTS**

*We would like to thank Spontaneous McKnight from Bio-Rad for the RiboGreen protocol adaptation used on the iCycler for cycling conditions compatible with fluorometer function. This material is based upon work supported by the Office of Research and Development, Medical Research Service, Department of Veterans Affairs, and the NIH/NIAAA.*

**REFERENCES**

1. **Bustin, S.** 2000. Absolute quantification of mRNA using real-time reverse transcription polymerase chain reaction assays. J. Mol. Endocrinol. *25*:169-193.
2. **Orlando, C., P. Pinzani, and M. Pazzagli.** 1998. Developments in quantitative PCR. Clin. Chem. Lab. Med. *36*:255-269.
3. **Peirson, S., J. Butler, and R. Foster.** 2003. Experimental validation of novel and conventional approaches to quantitative real-time PCR data analysis. Nucleic Acids Res. *31*:e73.
4. **Freeman, W., S. Walker, and K. Vrana.** 1999. Quantitative RT-PCR: pitfalls and potential. BioTechniques *26*:112-115.
5. **Jones, L., S. Yue, C. Cheung, and V. Singer.** 1998. RNA quantitation by fluorescence-based solution assay: RiboGreen reagent characterization. Anal. Biochem. *265*:368-374.
6. **Gonzalez, J. and C. Saiz-Jimenez.** 2003. Optical thermal cycler for use as a fluorimetric plate reader to estimate DNA concentrations. BioTechniques *34*:710-712.
7. **Kalajzic, Z., P. Liu, I. Kalajzic, Z. Du, A. Braut, M. Mina, E. Canalis, and D. Rowe.** 2002. Directing the expression of a green fluorescent protein transgene in differentiated osteoblasts: comparison between rat type I collagen and rat osteocalcin promoters. Bone *31*:654-660.
8. **Winer, J., C. Jung, I. Shackel, and P. Williams.** 1999. Development and validation of real-time quantitative reverse transcriptase-polymerase chain reaction for monitoring gene expression in cardiac myocytes in vitro. Anal. Biochem. *270*:41-49.
9. **Bustin, S.** 2002. Quantification of mRNA using real-time reverse transcription PCR (RT-PCR): trends and problems. J. Mol. Endocrinol. *29*:23-39.

Received 29 August 2003; accepted 14 October 2003.

*Address correspondence to Kristine M. Wiren, Portland VA Medical Center, P3-R&D39, 3710 SW US Veterans Hospital Road, Portland, OR 97239, USA. e-mail: wirenk@ohsu.edu*

# pTOC-KR: a positive selection cloning vector based on the ParE toxin

Han Geun Kim[1], Hyun Jin Hwang[1], Min Sung Kim[3], Dong Yun Lee[1], Sung Kyun Chung[1], Jung Min Lee[1,2], Ji Hyun Park[4], and Dae Kyun Chung[1,2,3]
*[1]Kyung Hee University, Suwon, Korea, [2]RNA Inc., Suwon, Korea, [3]DNA Inc., Seoul, Korea, and [4]University College London, London, UK*

*BioTechniques 36:60-64 (January 2004)*

Several prokaryotic cloning vectors have been developed to clone foreign DNA in bacteria. The insertion inactivation of β-galactosidase activity, for instance, is a common screening method of identifying recombinant DNA molecules in many vectors (1,2). However, this system poses several problems. For one, many vectors can self-ligate and give false transformants. Although β-galactosidase is widely used as a screening marker, it is limited to use with specially mutated *Escherichia coli* hosts for α-complementation. The color of the colonies is also hard to distinguish when the blue/white selection system is used. This system also requires expensive reagents: 5-bromo-4-chloro-3-indolyl-β-D-galactosidase (X-Gal) and isopropylthio-β-D-thiogalactopyranoside (IPTG).

To address these problems, several positive selection vector systems have been developed based on the toxin-antitoxin systems parD (Kis/Kid) of plasmid R1 (3) and on the CcdAB system of plasmid F (4). Similar positive selection cloning vectors using the transcriptional factor GATA-1 (5) or a cellulase gene (*CelA*) as screening marker (6) have also been developed. Nonetheless, the application of these systems is also limited; in most cases, they are host-limited and their cloning

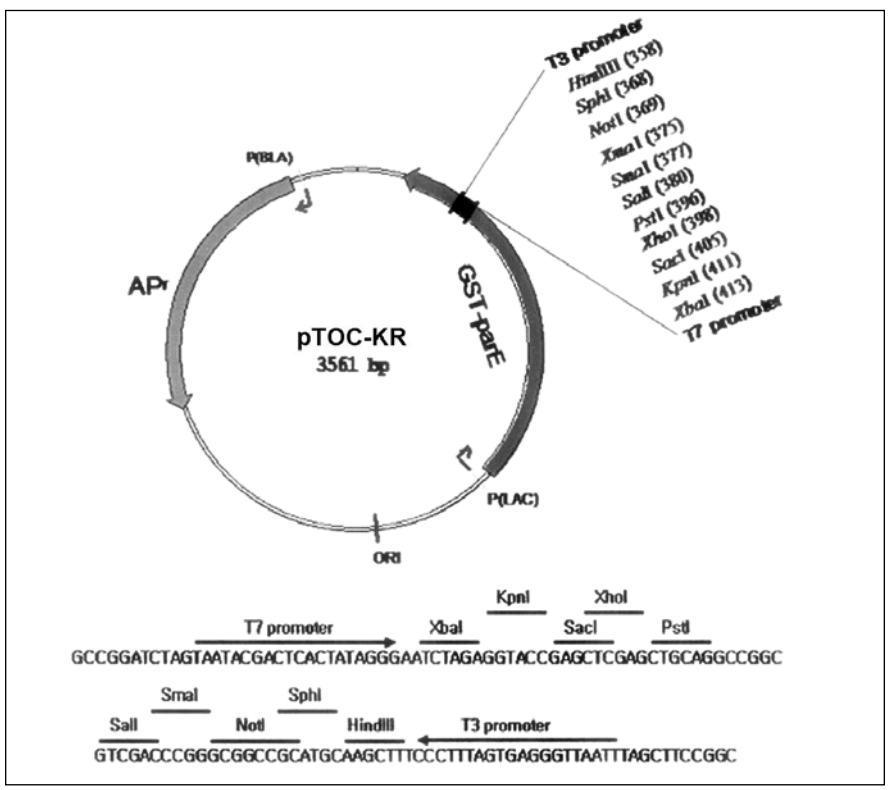


**Figure 1. Map of pTOC-KR.** The main feature of the vector is shown. Various multiple cloning sites and T7/T3 promoter sequences of the vector are represented.